Calculation of Permeability of Clay Mineral in Natural Slope by Using Numerical Analysis

Junghae Choi, Byung-gon Chae, Katsuyuki Kawamura, and Yasuaki Ichikawa

Abstract

A natural landslide is mainly occurred by rainfall, snowmelt, earthquakes and construction works. Especially, the role of rainfall or snowmelt in slope stability is very important because it causes a decrease in shear strength by reducing the soil cohesion. If clay exists in the weathered soil, the physical characteristics such as viscosity and permeability are generally different from the condition without the clay. In this case, changes of permeability or viscosity due to the rainfall or snowmelt are dependent on the content of clay in soil. In order to calculate the variation in permeability according to the content of clay in soil, many researchers have conducted laboratory experiments or in-situ tests in the field. However, it is difficult to determine the property of the clay such as a viscosity because of its poor crystalline property. In order to solve this problem and to calculate permeability of clay under various dry densities, we used molecular dynamic (MD) simulation to examine the viscosity of micro scale and homogenization analysis (HA) method to expand micro material property to macro scale. In this research, we determined the permeability of clay with various dry densities due to the rainfall or snowmelt conditions by using MD/HA method.

Keywords

Molecular dynamics • Homogenization analysis • Viscosity • Permeability • Clay

Molecular Structure of Kaolinite

Radioactive waste disposal facilities have been planned in formations containing kaolinite, for example in the Opalinus Clay of Switzerland, because of their low permeability and resultant diffusion-dominant characteristics. For safely isolating radioactive substances for a long time, it is essential to fully understand the physical and chemical properties of the host rock. For this purpose, authors here present a unified procedure of molecular dynamics (MD) simulation and homogenization analysis (HA) for water-saturated kaolinite clay. This MD/HA procedure was originally developed for analyzing seepage, diffusion and consolidation phenomena of bentonite clay. In the current research, a series of MD calculations were performed for kaolinite and kaolinite-water systems, appropriate to a saturated deep geological setting. Then, by using HA, the seepage behavior is determined for conditions of the spatial distribution of the water viscosity associated with some configuration of clay minerals. The seepage behavior is calculated for different void ratios and dry densities.

Kaolinite is a 1:1 clay mineral; composed of alternating silica tetrahedral and aluminum octahedral sheets. To achieve charge balance, the apical oxygens of the silica tetrahedra are incorporated into the octahedral sheet. In the plane of atoms common to both sheets, two-thirds of the

J. Choi (✉) • B.-g. Chae
Korea Institute of Geoscience and Mineral Resources, 124 Gwahang-no, Yuseong-gu, Daejeon 305-350, South Korea
e-mail: jhchoi@kigam.re.kr

K. Kawamura • Y. Ichikawa
Department of Urban Environmental Development, Okayama University, Okayama, Japan

K. Sassa et al. (eds.), *Landslide Science for a Safer Geoenvironment*, Vol. 2,
DOI 10.1007/978-3-319-05050-8_4,

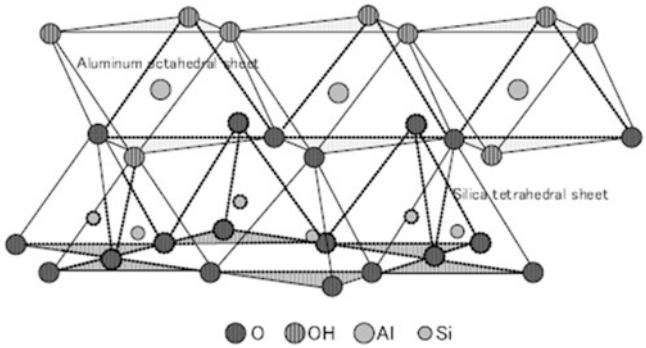

Fig. 1 Diagrammatic sketch of the structure of kaolinite

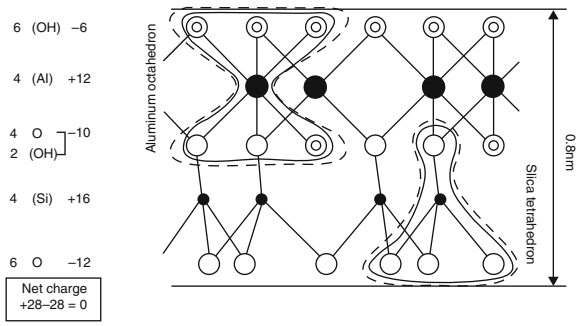

Fig. 2 Charge distribution in kaolinite

atoms are oxygens and are shared by both silicon and the octahedral aluminum cations. The remaining atoms in this plane comprise hydroxyl molecules (OH), located in such a way that each sheet is directly below the base of a silica tetrahedron. A diagrammatic sketch of the kaolinite structure is shown in Fig. 1. The structural formula is Si4Al4O10 $(OH)_8$, and the charge distribution is indicated in Fig. 2. Mineral particles of the kaolinite subgroup consist of these basic units, stacked in the c-direction. The bonding between successive layers is by both van der Waals forces and hydrogen bonds. The extensive hydrogen bonding, in particular, is sufficiently strong that there is no interlayer swelling. Because of a slight difference of oxygen-to-oxygen distance in the tetrahedral and octahedral layers there is some distortion of the ideal tetrahedral network. As a result, kaolinite is triclinic instead of monoclinic.

Homogenization Analysis for the Seepage

Seepage Problem by HA

A two-scale HA is introduced for a macro-domain Ω0 using the coordinate system x^0 and a micro-domain Ω1 using the coordinate system x^1. Both coordinates are related as $x = x^0/\varepsilon$ by the scale factor ε.

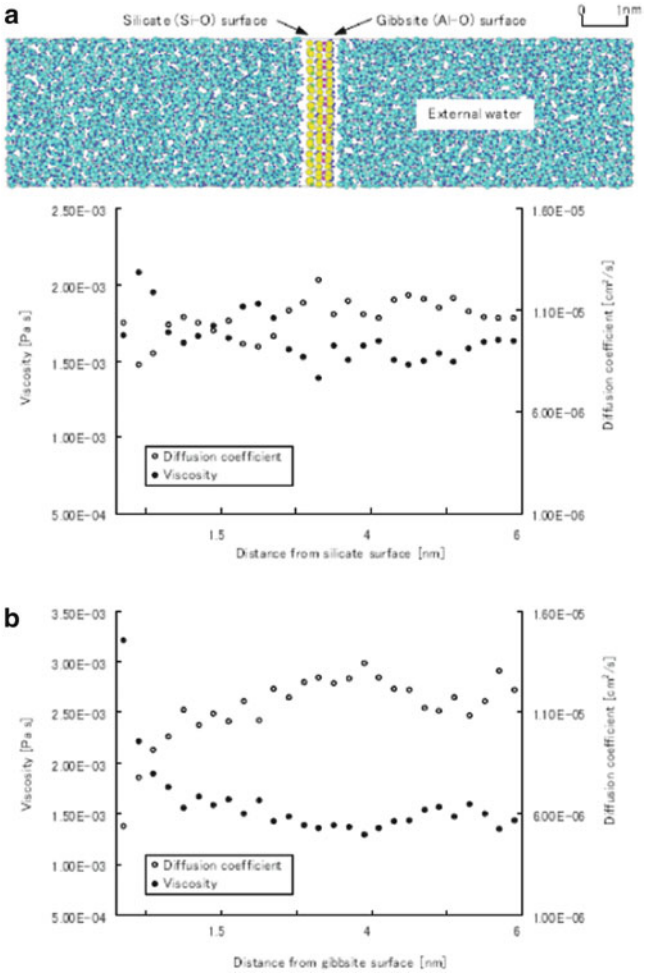

Fig. 3 Diffusivity and viscosity of water in the neighbourhood of a silicate surface (**a**) band gibbsite surface (**b**)

To represent incompressible flow, the following Stokes equation is introduced:

$$\rho\left(\frac{\partial V_i^\varepsilon}{\partial t} + V_j^\varepsilon \frac{\partial V_i^\varepsilon}{\partial x_j}\right) = -\frac{\partial P^\varepsilon}{\partial x_i} + \frac{\partial}{\partial x_j}\left(\eta \frac{\partial V_i^\varepsilon}{\partial x_j}\right) + f_i \quad \text{in} \quad \Omega_f \tag{1}$$

$$\frac{\partial V_i^\varepsilon}{\partial x_i} = 0 \quad \text{in} \quad \Omega_f \tag{2}$$

where ρ is the density of water, V^ε is the water velocity in the fluid domain Ω*f*, P^ε is the pressure, *fi* is the body force, and η is the water viscosity. Note that we consider a steady state, and hence the convective term $Vj\partial Vi/\partial xj$ of the left-hand side (LHS) of (1) vanishes in the perturbation procedure, and we can ignore the LHS terms from the beginning. The superscript ε implies a variable which varies rapidly in the microscale domain. The viscosity distribution calculated by MD is shown in Fig. 3 for an isolated kaolinite layer.

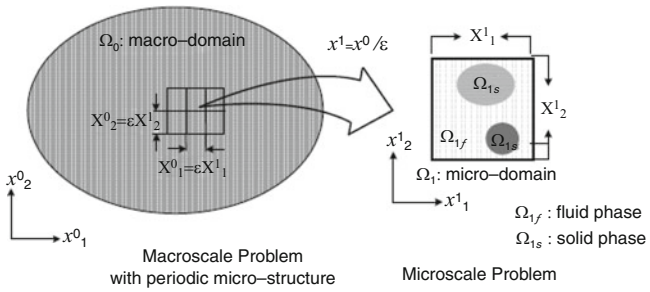

Fig. 4 Two-scale domains for homogenization analysis

Naturally the velocity vanishes on the fluid-solid interface Γ:

$$V_i^{\varepsilon} = 0 \quad \text{on} \quad \Gamma \tag{3}$$

Now we introduce 'two-scale domains'for homogenization analysis (Fig. 4); that is, the macro-domain Ω0 and micro-domain Ω1. Coordinate systems that were set x^0 in Ω0 and x^1 in Ω1 which are related by

$$x^1 = \frac{x^0}{\varepsilon} \tag{4}$$

Since the two-scale coordinates are employed, the differentiation is changed to

$$\frac{\partial}{\partial x_i} = \frac{\partial}{\partial x_i^0} + \frac{1}{\varepsilon}\frac{\partial}{\partial x_i^1} \tag{5}$$

By using the parameter ε we introduce the following perturbations:

$$\begin{aligned} V_i^{\varepsilon}(x) &= \varepsilon^2 V_i^0\left(x^0, x^1\right) + \varepsilon^3 V_i^1\left(x^0, x^1\right) + \ldots \\ P^{\varepsilon}(x) &= P^0\left(x^0, x^1\right) + \varepsilon P^1\left(x^0, x^1\right) + \ldots \end{aligned} \tag{6}$$

The perturbed terms of the right-hand sides (RHS) of (6) are assumed to be periodic:

$$\begin{aligned} V_i^{\alpha}(x^0, x^1) &= V_i^{\alpha}\left(x^0, x^1 + X^1\right) \\ P^{\alpha}(x^0, x^1) &= P^{\alpha}\left(x^0, x^1 + X^1\right) \end{aligned} \tag{7}$$

where $\boldsymbol{X}^1$ is the size of a microscale unit cell.

Equations (5) and (6) were substituted into (1) and (2) to get a set of perturbation equations. Due to the ε^{-1}-term resulting from (1) we understand that p^0 is a function of only the macro-coordinates $\boldsymbol{x}^0$. The ε^0-term resulted from (1) is given by

$$-\frac{\partial P^1}{\partial x_i^1} + \frac{\partial}{\partial x_j^1}\left(\eta \frac{\partial V_i^0}{\partial x_j^1}\right) = \frac{\partial P^0}{\partial x_i^0} - f_i \tag{8}$$

The body force $\boldsymbol{f}$ usually works in the macro-domain Ω0 ($f = f(x^0)$), and the RHS terms of (8) are functions only of x^0. Thus we can introduce the separation of variables into $p^1(x^0, x^1)$ and $V^0(x, x^1)$ as

$$\begin{aligned} V_i^0(x^0, x^1) &= -\left|\frac{\partial P^0(x^0)}{\partial x_j^0} - f_j(x^0)\right| v_i^j(x^1) \\ P^1(x^0, x^1) &= -\left|\frac{\partial P^0(x^0)}{\partial x_j^0} - f_j(x^0)\right| p^j(x^1) \end{aligned} \tag{9}$$

These are substituted into (8), and we get the following *microscale incompressible Stokes' equations*:

$$\begin{aligned} &-\frac{\partial P^k}{\partial x_i^1} + \frac{\partial}{\partial x_j^1}\left(\eta \frac{\partial v_i^k}{\partial x_j^1}\right) + \delta_{ik} = 0 \quad \text{in} \quad \Omega_{1f} \\ &\frac{\partial v_i^k}{\partial x_j^1} = 0 \quad \text{in} \quad \Omega_{1f} \end{aligned} \tag{10}$$

where $v(x^1)$ and $p^k(x^1)$ are characteristic functions for velocity and pressure, respectively (δ_{ik} is Kronecker's delta). By solving (10) under periodic conditions the characteristic functions, which reflect a complex geometry of the microscale domain, were obtained. Let us operate an integral average of (9) in the micro-domain, producing Darcy's law as,

$$\begin{aligned} \widetilde{V}_i^0(x^0) &= \left\langle V_i^0(x^0, x^1)\right\rangle = -K_{ji}\left|\frac{\partial P^0(x^0)}{\partial x_j^0} - f_j(x^0)\right| \\ K_{ij} &\equiv \left\langle V_j^i(x^1)\right\rangle = \frac{1}{|\Omega_1|}\int_{\Omega_{1f}} V_j^i(x^1)\, dx^1 \end{aligned} \tag{11}$$

where $|\Omega_1|$ is the volume of the micro-domain Ω1 and represents an averaging operation in the micro-domain. We call K_{ij} the HA-permeability.

Equation (8) gives a mass conservation relationship between the micro-domain and the macro-domain. When averaging this in the micro-domain, the second term of LHS vanishes due to the periodicity; then substituting Darcy's law (9) yields the *macroscale incompressible permeability equation*:

$$\frac{\partial \widetilde{V}_i^0}{\partial x_i^0} = 0 \Rightarrow -\frac{\partial}{\partial x_i^0}\left[-K_{ji}\left\{\frac{\partial P^0(x^0)}{\partial x_j^0} - f_j(x^0)\right\}\right] = 0 \tag{12}$$

The water velocity and pressure are approximated as

$$V_i^{\varepsilon}(x^0) \simeq \varepsilon^2 V_i^0(x^o, x^1), \qquad P^{\varepsilon}(x^o) \simeq P^0(x^o) \tag{13}$$

It should be remembered that, in HA, the distribution of velocity and pressure are calculated in the micro-domain. The procedure to solve the total HA-seepage problem is

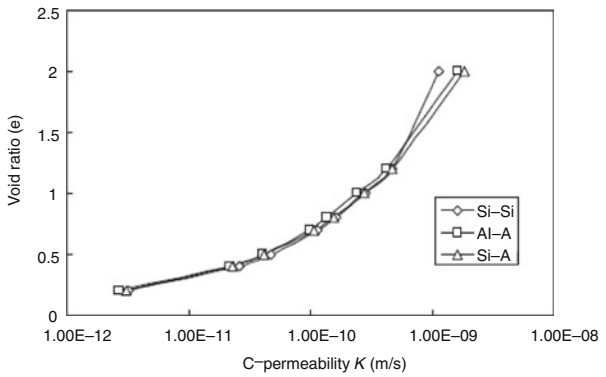

Fig. 5 Relationship between C-permeability (K^*) and void ratio (e)

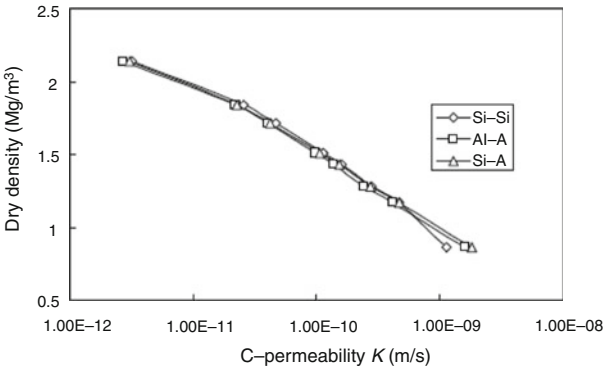

Fig. 6 Relationship between C-permeability (K^*) and dry density (ρ_d)

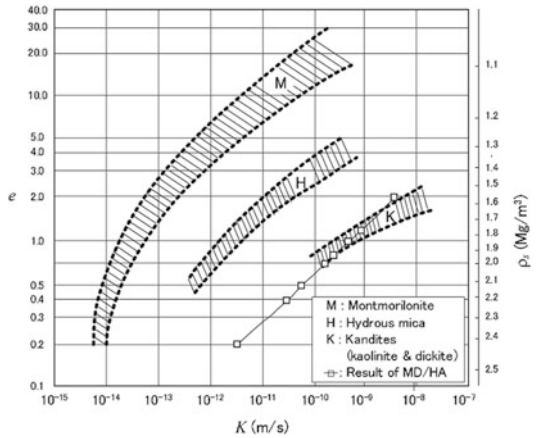

Fig. 7 Permeabilities given by HA and by Pusch

summarized as follows: first, we solve micro-scale equation (10) and get V_i^k and P^k, then determine Darcy's coefficient K_{ij} from (11). Next by solving macro-scale equation (12), we get the macro-pressure and velocity fields. In classical geomechanics, Darcy's law is written as

$$\hat{V}_i^* = -K_{ij}^* \frac{\partial \phi}{\partial x_j^0}, \quad \phi = \frac{p}{\rho g} + \xi \tag{14}$$

Where ϕ is the total head, $p/\rho g$ is the pressure head, ξ is the elevation head, and g is the gravity constant. K_{ij}^* is called C-permeability and is defined as

$$K_{ij}^* = \varepsilon^2 \rho g K_{ij} \tag{15}$$

Conclusions

Macroscale and microscale models of the kaolinite-water permeability system analyzed here are shown in Fig. 7. The number of mineral layers in one stack is assumed to be eight. It is known that one layer is connected to others by hydrogen bond, and the separation distance is calculated as 0.8 nm by the MD simulation. The density of solid part of the mineral is also calculated by MD as 2.56 g/cm^3. A distribution of viscosity calculated by MD is shown in Fig. 3. The distance between two stacks is determined by the overall dry density of clay. We assume that the kaolinite stacks are randomly distributed; then the averaged permeability K* is estimated as $K^* = K_{11}^*/3$. The relationships between the C-permeability (K^*), the void ratio (e) and the dry density (ρ_d) are plotted in Figs. 5 and 6. These relations can curve fit as

$$\begin{aligned} \log K^* &= 1 \times 10^{-9} \rho_d^{-6.709} \\ \log K^* &= 3 \times 10^{-10} e^{2.775} \end{aligned} \tag{16}$$

where the unit of K* is in m/s.

In this paper, a unified MD/HA method for analyzing the seepage problem in kaolinite was presented. The results obtained by this method are similar to the experimental data, which supports the validity of the method (Fig. 7).

Acknowledgments This research was supported by the Public Welfare & Safety Research Program through the National Research Foundation of Korea (NRF) funded by the Ministry of Science, ICT & Future Planning (2012M3A2A1050983).

References

Delville A (1995) Monte Carlo simulations of surface hydration: an application to clay wetting. J Phys Chem 99:2033–2037

Delville A, Sokolowski A (1993) Adsorption of vapor at a solid interface: a molecular model of clay wetting. J Phys Chem 97:6261–6271

Du J, Cormack AN (2004) The medium range structure of sodium silicate glasses: a molecular dynamics simulation. J Non-Cryst Solids 349:66–79

Ichikawa Y, Kawamura K, Nakano M, Kitayama K, Kawamura H (1999) Unified molecular dynamics and homogenization analysis

for bentonite behaviour: current results and the future possibility. Eng Geol 54:21–31

Ichikawa Y, Kawamura K, Nakano M, Kitayama K, Seiki T, Theramast N (2001) Seepage and consolidation of bentonite saturated with pure-or salt-water by the method of unified molecular dynamics and homogenization analysis. Eng Geol 60:127–138

Kawamura K, Ichikawa Y (2001) Physical properties of clay minerals and water -By means of molecular dynamics simulations. Bull Earthq Res Inst Univ Tokyo 76:311–320

Kawamura K, Ichikawa Y, Nakano M, Kitayama K, Kawamura H (1999) Swelling properties of smectite up to 90C: In situ X-ray diffraction experiments and molecular dynamics simulations. Eng Geol 54:75–79

Salles J, Thovert JF, Delannay R, Prevors L, Auriault JL, Adler PM (1993) Taylor dispersion in porous media. Determination of the dispersion tensor. Phys Fluids A5(10):23482376

Skipper NT, Sposito G, Chang FRC (1995) Monte Carlo simulation of interlayer molecular structure in swelling clay minerals: 2. Monolayer hydrates. Clays Clay Miner 43(3):294–303